Cell Death and Differentiation (2017) 24, 26–37
Official journal of the Cell Death Differentiation Association
www.nature.com/cdd

OPEN

Coordinated ubiquitination and phosphorylation of RIP1 regulates necroptotic cell death

M Cristina de Almagro[1,7,8], Tatiana Goncharov[1,8], Anita Izrael-Tomasevic[2], Stefanie Duttler[1], Matthias Kist[1], Eugene Varfolomeev[1], Xiumin Wu[3], Wyne P Lee[3], Jeremy Murray[4], Joshua D Webster[5], Kebing Yu[2], Donald S Kirkpatrick[2], Kim Newton[6] and Domagoj Vucic*[,1]

Proper regulation of cell death signaling is crucial for the maintenance of homeostasis and prevention of disease. A caspase-independent regulated form of cell death called necroptosis is rapidly emerging as an important mediator of a number of human pathologies including inflammatory bowel disease and ischemia–reperfusion organ injury. Activation of necroptotic signaling through TNF signaling or organ injury leads to the activation of kinases receptor-interacting protein kinases 1 and 3 (RIP1 and RIP3) and culminates in inflammatory cell death. We found that, in addition to phosphorylation, necroptotic cell death is regulated by ubiquitination of RIP1 in the necrosome. Necroptotic RIP1 ubiquitination requires RIP1 kinase activity, but not necroptotic mediators RIP3 and MLKL (mixed lineage kinase-like). Using immunoaffinity enrichment and mass spectrometry, we profiled numerous ubiquitination events on RIP1 that are triggered during necroptotic signaling. Mutation of a necroptosis-related ubiquitination site on RIP1 reduced necroptotic cell death and RIP1 ubiquitination and phosphorylation, and disrupted the assembly of RIP1 and RIP3 in the necrosome, suggesting that necroptotic RIP1 ubiquitination is important for maintaining RIP1 kinase activity in the necrosome complex. We also observed RIP1 ubiquitination in injured kidneys consistent with a physiological role of RIP1 ubiquitination in ischemia–reperfusion disease. Taken together, these data reveal that coordinated and interdependent RIP1 phosphorylation and ubiquitination within the necroptotic complex regulate necroptotic signaling and cell death.
Cell Death and Differentiation (2017) **24,** 26–37; doi:10.1038/cdd.2016.78; published online 12 August 2016

Regulated cell death has a critical role in development and homeostasis in metazoans.[1] Abnormalities in cell death pathways have been linked to a variety of human diseases including cancer, neurodegeneration, tissue damage and immune disorders.[2] Apoptosis is the best-known form of regulated cell death and it relies on the activation of cysteine proteases called caspases.[3] Necroptosis is an alternative form of regulated cell death, which has recently been linked to various human health conditions.[4] Unlike apoptosis, necroptosis occurs when caspases are inhibited and it involves activation of receptor-interacting protein kinase 1 (RIP1; RIPK1) and receptor-interacting protein kinase 3 (RIP3; RIPK3).[5] Necroptosis can be initiated by TNF*α* (tumor necrosis factor *α*) and a few related TNF family ligands, TLR3 and 4 (toll-like receptors), tissue damage or certain viruses.[6]

TNF binding to TNF receptor 1 (TNFR1) can activate nuclear factor-*κ*B (NF-*κ*B) and mitogen-activated protein kinase (MAPK) signaling by recruiting the E3 ligases c-IAP1 and 2 (cellular inhibitors of apoptosis 1 and 2) and their substrate RIP1.[7] Ubiquitination of RIP1 and the c-IAPs nucleates the formation of receptor-associated signaling complex-I, which includes the IKK (inhibitor of *κ*B kinase) complex and LUBAC (linear ubiquitin chain assembly complex).[7–11] Assembly of diverse ubiquitin chain linkages on RIP1 is postulated to facilitate the retention of RIP1 within complex-I.[8,12,13] In addition to stimulation of NF-*κ*B and MAPK signaling, TNF can also trigger cell death by inducing the formation of cytoplasmic apoptosis and necroptosis-inducing complexes IIa and IIb.[5,14] Complex IIa promotes caspase-8 activation, whereas complex IIb (also called the necrosome) forms when caspase-8 is inhibited and involves RIP1-mediated recruitment of RIP3, leading to the activation of RIP3 kinase activity.[5] RIP3 phosphorylates pseudokinase mixed lineage kinase-like (MLKL) prompting MLKL oligomerization, membrane translocation and cell rupture.[15–18]

Diverse necroptotic stimuli converge on the activation of RIP1 and RIP3 kinases.[5,19,20] Thus, it is not surprising that necroptotic cell death signaling can be regulated through the modulation of RIP1 and RIP3 kinase activities.[21] However, additional pathway regulation can be accomplished by other post-translational modifications such as ubiquitination.[22] Ubiquitination, a process by which proteins are covalently

[1]Department of Early Discovery Biochemistry, Genentech, 1 DNA Way, South San Francisco, CA 94080, USA; [2]Department of Protein Chemistry, Genentech, 1 DNA Way, South San Francisco, CA 94080, USA; [3]Department of Translational Immunology, Genentech, 1 DNA Way, South San Francisco, CA 94080, USA; [4]Department of Structural Biology, Genentech, 1 DNA Way, South San Francisco, CA 94080, USA; [5]Department of Pathology, Genentech, 1 DNA Way, South San Francisco, CA 94080, USA and [6]Departments of Physiological Chemistry, Genentech, 1 DNA Way, South San Francisco, CA 94080, USA
*Corresponding author: D Vucic, Early Discovery Biochemistry, Genentech, 1 DNA Way, South San Francisco 94080, California, USA. Tel: +1 650 225 8839; Fax: +1 650 225 6127; E-mail: domagoj@gene.com
[7]Current address: Laboratorios Ordesa SL, Parc Científic de Barcelona, Barcelona, Spain.
[8]These authors share the first authorship.

Abbreviations: RIP1, receptor-interacting protein 1; RIP3, receptor-interacting protein 3; TNF, tumor necrosis factor; IAP, inhibitor of apoptosis; MLKL, mixed lineage kinase-like; FADD, Fas-associated death domain; NF-*κ*B, nuclear factor-*κ*B; JNK, Jun N-terminal kinase; MEF, mouse embryonic fibroblast; BMDM, bone marrow-derived macrophage; BUN, blood urea nitrogen; MAPK, mitogen-activated protein kinase; IRI, ischemia–reperfusion injury; IL-8, interleukin-8

Received 12.2.16; revised 15.6.16; accepted 07.7.16; Edited by RA Knight; published online 12.8.16

modified with the protein ubiquitin, can regulate protein stability, subcellular localization or stimulate various signaling pathways.[23] On the one hand, TNF-induced NF-κB signaling is a prime example of a signaling pathway that is tightly regulated by ubiquitination mediated by c-IAP proteins and LUBAC.[14,24] On the other hand, TNF-mediated apoptotic cell death is only indirectly affected by ubiquitination because it requires deubiquitination of RIP1.[25] Contrary to apoptosis, necroptotic cell death signaling involves the ubiquitination of key necroptosis components.[26–29]

In this study, we have examined the functional significance of necroptotic RIP1 ubiquitination. We have established the critical role of RIP1 kinase activity for RIP1 ubiquitination in cells undergoing necroptosis. Using an antibody that selectively recognizes phosphorylated RIP1, we show concomitant phosphorylation and ubiquitination of RIP1 within the necrosome complex. Analyses of these ubiquitination events using immunoaffinity enrichment and mass spectrometry revealed multiple endogenous ubiquitination events that are specific to necroptotic signaling. Mutation of the K115 ubiquitination site on RIP1 reduced necroptotic cell death, RIP1 phosphorylation and proper necrosome assembly, suggesting that necroptotic RIP1 ubiquitination has an important role in maintaining RIP1 kinase activity in the necrosome complex. Finally, RIP1 ubiquitination was also observed in the kidneys of mice following renal injury consistent with a physiological role for this post-translational modification of RIP1 in ischemia–reperfusion disease.

Results

Necroptotic RIP1 ubiquitination occurs in the absence of MLKL or RIP3. TNF signaling triggers RIP1 ubiquitination within TNFR1-associated signaling complex I, which has an important role in the activation of NF-κB and MAPK signaling, leading to proinflammatory gene expression.[7,8] TNF can also trigger the formation of cell death-promoting apoptotic and necroptotic protein complexes.[7] Interestingly, RIP1 was found to be ubiquitinated during necroptotic signaling in human and mouse cells.[26] We have confirmed those findings and show that induction of necroptosis in human HT29 cells by the combination of TNF, pancaspase inhibitor zVAD and IAP antagonist BV6 (TBZ) stimulates RIP1 ubiquitination within the necrosome, whereas induction of apoptosis does not (TNF plus BV6, TB treatment) (Figure 1a and Supplementary Figure S1A). We have further analyzed the assembly of necroptotic cell death complex in HT29 cells treated with TBZ for 1, 2 and 4 h by using gel filtration analysis (Figure 1b). Stimulation of cells with TBZ triggered translocation of RIP1, RIP3, caspase-8, FADD (Fas-associated death domain) and MLKL to large multiprotein complexes, which was accompanied by RIP1, RIP3 and MLKL phosphorylation (Figure 1b). Furthermore, accumulation of phosphorylated RIP1 coincided with RIP1 ubiquitination (Figure 1b), suggesting that these two post-translational modifications of RIP1 overlap in the necroptotic signaling complex.

Given that the kinase RIP3 and pseudokinase MLKL have critical roles in mediating necroptotic cell death (Supplementary Figure S1B), we explored their relevance for RIP1 ubiquitination. Treatment of wild-type (WT), *Mlkl*$^{-/-}$- or *Rip3*$^{-/-}$-immortalized mouse embryonic fibroblasts (MEFs) with the necroptotic stimulus TBZ triggered comparable RIP1 ubiquitination (Figure 1c). Furthermore, investigation of the necrosome in MEF cells also revealed comparable RIP1 ubiquitination in the necroptotic complex containing RIP3 and FADD in WT, *Mlkl*$^{-/-}$ or *Rip3*$^{-/-}$ MEFs (Supplementary Figure S1C). Conversely, ectopic expression of RIP3 in human HT1080 cells, which normally do not express RIP3, did not affect TBZ-induced RIP1 ubiquitination (Supplementary Figure S1D). In addition, treatment of HT29 cells with the RIP3 kinase inhibitor GSK843 did not affect TBZ-stimulated RIP1 ubiquitination and phosphorylation, but it blocked MLKL phosphorylation, thus confirming the antinecroptotic activity of GSK843 (Figure 1d). Finally, knockdown of RIP3 or MLKL in HT29 cells did not obstruct TBZ-induced RIP1 ubiquitination either (Supplementary Figure S1E). Thus, necroptosis-induced RIP1 ubiquitination does not require execution of necroptotic cell death.

RIP1 kinase activity regulates ubiquitination of RIP1 in necroptosis. To investigate the importance of RIP1 kinase activity for necroptotic RIP1 ubiquitination, we treated HT29 cells with TBZ in the presence of different RIP1 kinase inhibitors (Nec-1, Nec-1Cl and Nec-4). Treatment with these necrostatin compounds prevented TBZ-induced RIP1 phosphorylation and ubiquitination (Figure 2a). Inactivation of RIP1 kinase activity prevents the execution of necroptotic cell death without affecting TNF-stimulated NF-κB and MAPK activation (Figures 2b–e and Supplementary Figure S2A).[21] Following TBZ treatment, we observed RIP1 ubiquitination in primary macrophages isolated from WT animals but not from *Rip1*$^{KD/KD}$ knock-in mice expressing catalytically inactive RIP1 D138N (Figure 2b). Similarly, induction of necroptosis triggered K63- and linear chain-linked RIP1 ubiquitination in WT immortalized MEFs, whereas it was greatly reduced in *Rip1*$^{KD/KD}$ cells (Figure 2e). Given that inactivation or inhibition of RIP1 kinase activity blocks association of RIP1 with RIP3 and caspase-8 into the necrosome complex (Supplementary Figures S2B and C),[30,31] these data are consistent with the critical importance of RIP1 kinase activity for its necroptotic ubiquitination in the necrosome.

Furthermore, by examining the caspase-8-associated necrosome complex, we observed concomitant recruitment of phosphorylated and ubiquitinated RIP1 into the necroptotic complex (Figure 2f). Interestingly, the appearance of phosphorylated RIP1 in cellular lysates coincided with recruitment of phosphorylated RIP1 into the necrosome (Figure 2f). However, TNF alone, or in combination with BV6 to induce apoptosis, did not stimulate RIP1 phosphorylation or association of phosphorylated RIP1 with caspase-8 (Figure 2f). The appearance of phosphorylated RIP3 in the necrosome and consequent MLKL phosphorylation were delayed relative to RIP1 phosphorylation (Figures 2f and 1b), indicating that RIP1 phosphorylation in the necrosome precedes the activation of RIP3 kinase activity. Collectively, these data suggest that phosphorylation and ubiquitination of RIP1 coincide with its engagement in the necrosome, leading to recruitment and activation of RIP3 and execution of necroptotic cell death.

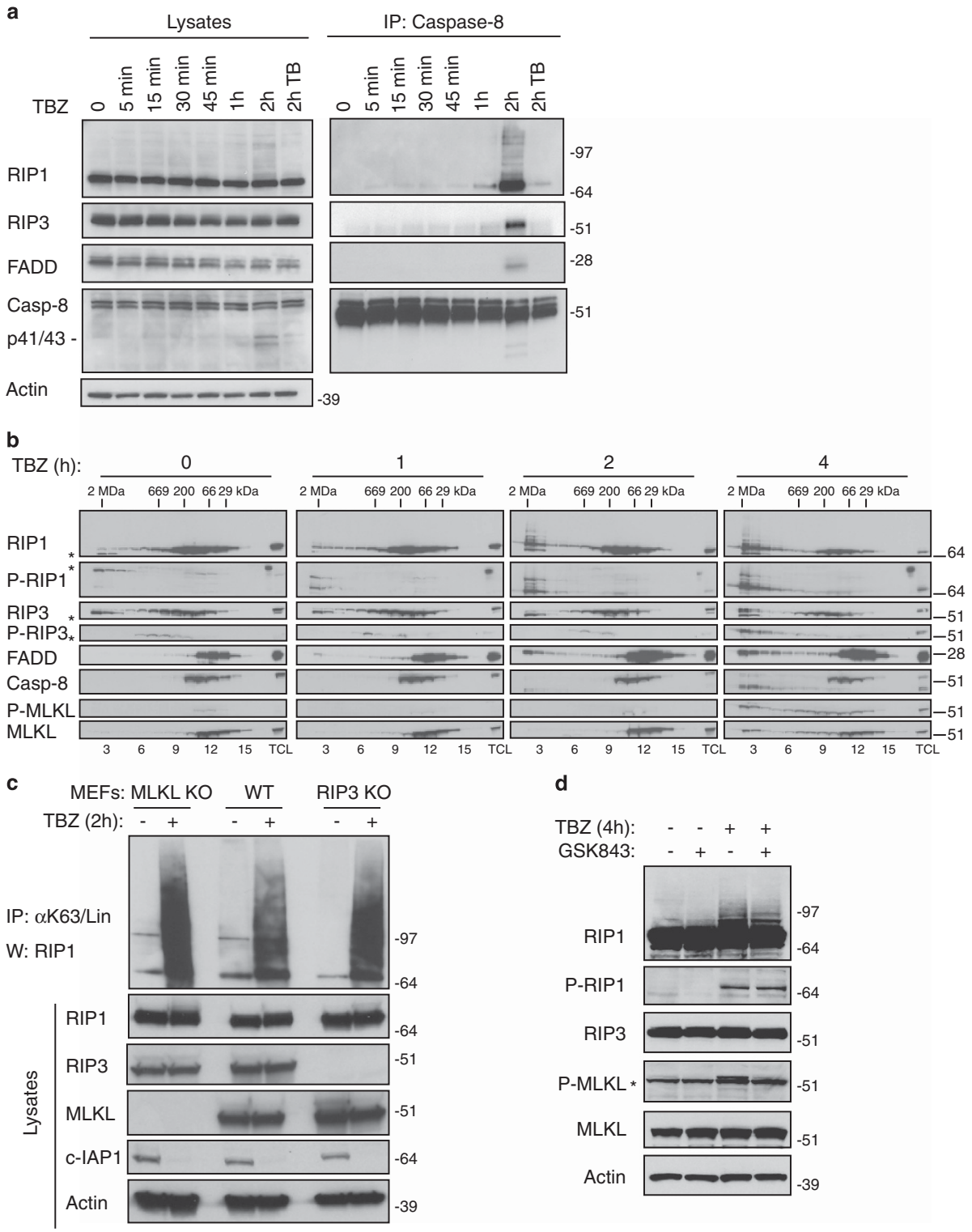

Figure 1 RIP1 is ubiquitinated during necroptotic signaling independently of RIP3 and MLKL. (**a**) HT29 cells were treated for the indicated periods of time with TNFα 20 ng/ml (T), BV6 2 μM (B) and zVAD 20 μM (Z). Cell lysates were immunoprecipitated with caspase-8 antibody. The pull-downs and lysates were analyzed by western blotting with the indicated antibodies. (**b**) HT29 cells were treated with TBZ as in (**a**) for the indicated times. Lysates were fractionated on a Superose 6 10/300 GL column and the resulting fractions as well as total cell lysates were separated by SDS-PAGE and probed with the indicated antibodies. Asterisks denote nonspecific bands. Fraction numbers are indicated below and molecular weight markers on top of western blots. (**c**) WT, MLKL KO or RIP3 KO MEFs were treated for 2 h with TNFα 100 ng/ml (T), BV6 2 μM (B) and zVAD 20 μM (Z) as indicated. Cells were lysed in 6 M urea buffer, immunoprecipitated using linear and K63 linkage-specific anti-ubiquitin antibodies and analyzed by western blotting with the indicated antibodies. (**d**) HT29 cells were treated for 4 h with TNFα 10 ng/ml (T), BV6 0.5 μM (B) and zVAD 20 μM (Z) in the absence or presence of GSK843 (10 μM). Cell lysates were analyzed by western blotting with the indicated antibodies. Asterisk denotes lower nonspecific band

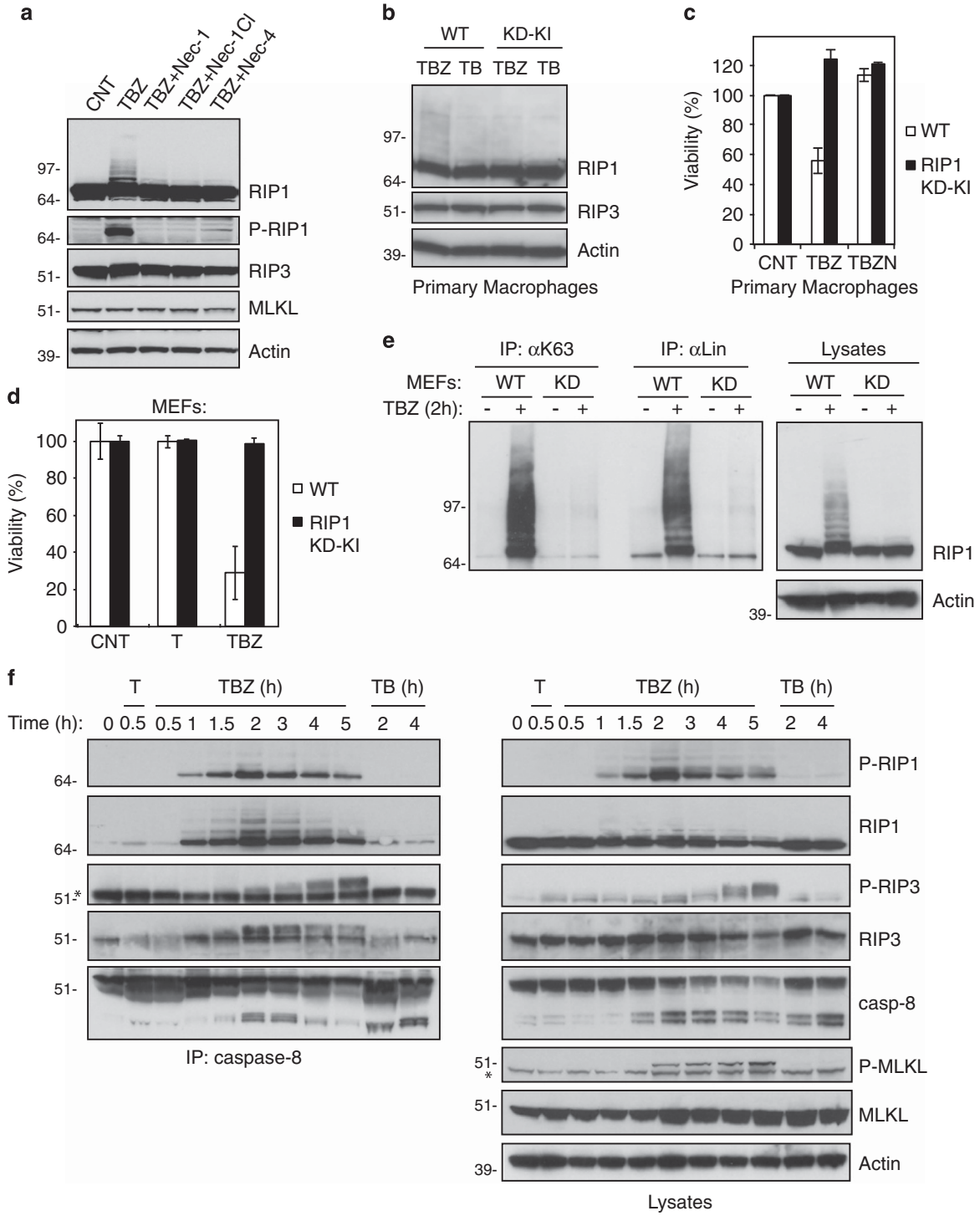

Figure 2 RIP1 kinase activity regulates RIP1 ubiquitination. (**a**) HT29 cells were treated for 3 h with TNFα 10 ng/ml (T), BV6 0.5 μM (B), zVAD 20 μM (Z) and necrostatin compounds 30μM (N) as indicated. Cell lysates were analyzed by western blotting with the indicated antibodies. (**b**) Primary BMDMs were treated for 2 h with TNFα 100ng/ml (T), BV6 2 μM (B) and zVAD 20 μM (Z) as indicated. Cell lysates were analyzed by western blotting with the indicated antibodies. (**c**) Primary BMDMs were treated for 24 h with TNFα 100 ng/ml (T), BV6 2 μM (B), zVAD 20 μM (Z) and Nec-1 30 μM (N) as indicated. Cell viability was assessed by CellTiter-Glo (Promega). Data are mean $\pm$ S.E.M. values of four experiments. (**d**) WT or RIP1 kinase-dead knock-in (RIP1 KD-KI) MEFs were treated for 24 h with TNFα 100 ng/ml (T), BV6 2 μM (B) and zVAD 20 μM (Z) as indicated. Cell viability was assessed by CellTiter-Glo. Data are mean $\pm$ S.E.M. values of four experiments. (**e**) WT or RIP1 KD MEFs were treated for 2 h as in (**d**). Cells were lysed in 6 M urea buffer, immunoprecipitated using linear or K63 linkage-specific anti-ubiquitin antibodies and analyzed by western blotting with the indicated antibodies. (**f**) HT29 cells were treated for indicated time points with TNFα 20 ng/ml (T) alone or in combination with BV6 2 μM (TB), or with BV6 and zVAD 20 μM (TBZ). Cell lysates were immunoprecipitated with caspase-8 antibody. The pull-downs and lysates were analyzed by western blotting with the indicated antibodies. Asterisks denote lower nonspecific bands

Analyses of ubiquitination in necroptotic signaling. To elucidate how TNF-mediated cell death pathways modulate cellular ubiquitination, we treated HT29 cells with TNF and BV6 alone, or in combination with zVAD and necrostatin-1 (Figures 3a and Supplementary Figure S3A). Changes in ubiquitination levels caused by different treatment

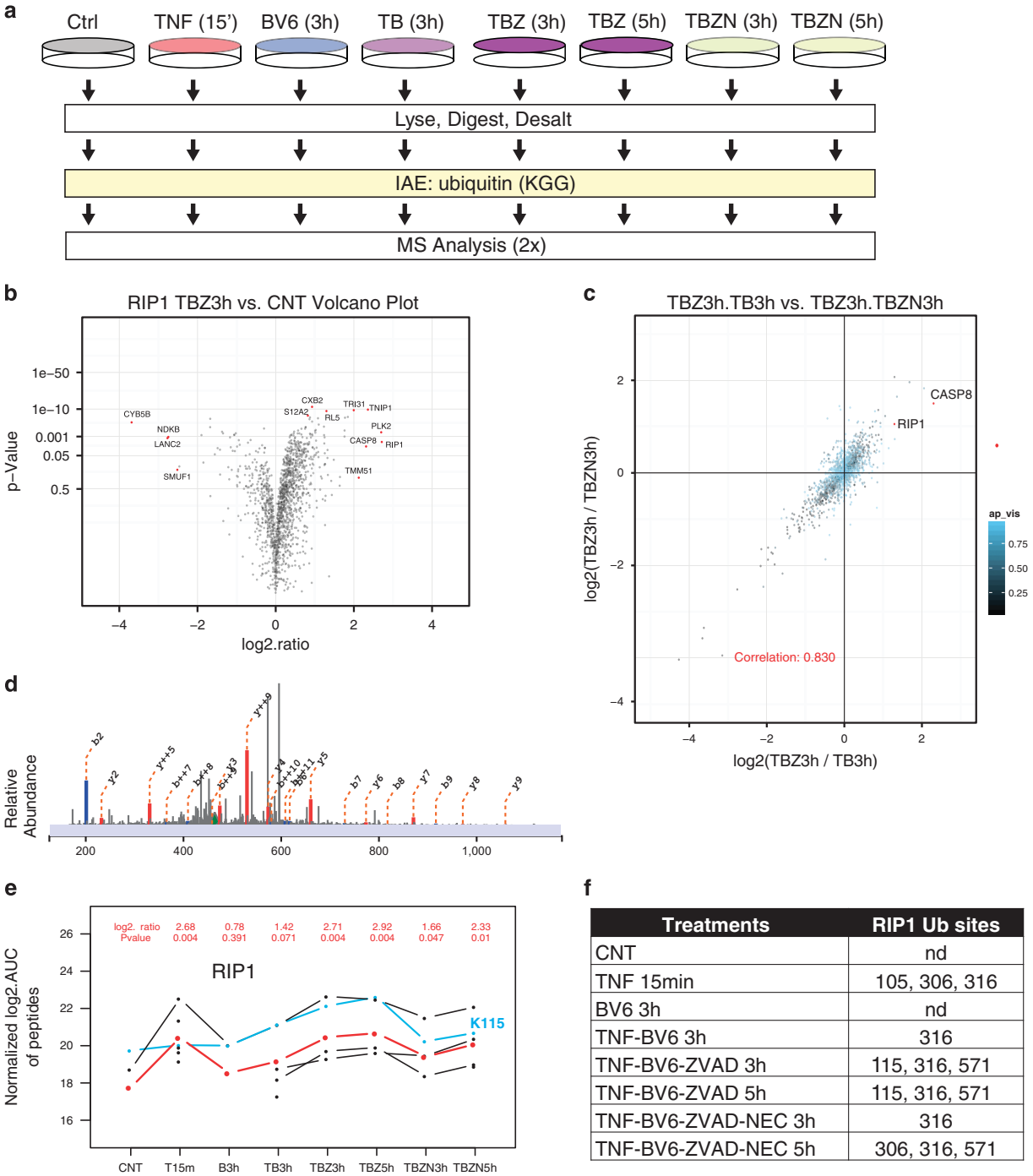

f

Treatments	RIP1 Ub sites
CNT	nd
TNF 15min	105, 306, 316
BV6 3h	nd
TNF-BV6 3h	316
TNF-BV6-ZVAD 3h	115, 316, 571
TNF-BV6-ZVAD 5h	115, 316, 571
TNF-BV6-ZVAD-NEC 3h	316
TNF-BV6-ZVAD-NEC 5h	306, 316, 571

Figure 3 Analyses of ubiquitination in HT29 cells in necroptotic signaling. (**a**) MS analysis of ubiquitin remnant K-GG peptides in HT29 cells treated with TNFα 20 ng/ml (T), BV6 2 μM (B) and zVAD 20 μM (Z) in the absence or presence of Nec-1 (N) as indicated. (**b**) Volcano plot of the log 2-based ratio of K-GG peptide abundance for proteins between TBZ 3 h and control conditions. Peptide level data were aggregated at the protein level and *P*-values were generated by linear mixed-effect (LiME) modeling. Selected proteins are highlighted in red. (**c**) Scatterplot and Pearson's correlation of K-GG abundance ratios for the effect of adding Nec-1 compared with removing zVAD in the TBZ condition showing that changes in K-GG peptide abundance are highly correlated with one another. Among all affected proteins, RIP1 and caspase-8 show substantial upregulation in ubiquitination level. (**d**) MS/MS spectrum showing identification of representative K-GG peptide demonstrating ubiquitination of RIP1 at Lys115. (**e**) LiME plot of K-GG peptides from RIP1 protein across eight conditions. Black lines correspond to AUC abundance measurements from confidently matched K-GG peptides. LiME model output at the protein level is shown in red. Log 2 ratios and *P*-values are reported for each treatment relative to the control. The ubiquitinated peptide corresponding to Lys115 is colored in blue. (**f**) RIP1 ubiquitination sites identified directly by PSMs in each condition. ND stands for none detected

combinations were quantified by LC-MS/MS using the K-GG ubiquitin remnant profiling workflow (Figure 3a). After applying defined treatment conditions, protein lysates were proteolytically digested into peptides. Ubiquitinated peptides with the diglycine remnant were subsequently enriched by anti-K-ε-GG antibody and MS analysis was performed to acquire site-specific ubiquitination events under each condition. In total, $>10\,000$ unique K-GG peptides were identified from $>101\,000$ K-GG peptide spectral matches (PSMs) with false discovery rates of 0.23% and 1.92% at the PSM and protein level, respectively (Supplementary Table 1). Each PSM was quantified by the peak area under the curve and summarized to the protein level using a linear mixed-effect model (Supplementary Table 2). Cotreatment with TBZ increased ubiquitination of a set of proteins, including RIP1, caspase-8, TNFAIP3-interacting protein 1 (TNIP1) and E3 ubiquitin-protein ligase TRIM31 (Figure 3b). Interestingly, adding Nec-1 or removing zVAD from the TBZ treatment group overall has a similar effect (Figure 3c, Pearson's correlation score: 0.830), but RIP1 and caspase-8 showed significant changes. In the conditions explored in this experiment, RIP1 ubiquitination was significantly increased after adding TNF for 15 min (log 2 ratio = 2.68 *versus* control, *P*-value: 0.004), whereas BV6 reduced TNF-induced RIP1 ubiquitination (log 2 ratio = 1.42 *versus* control, *P*-value: 0.071) (Figures 3d and e). Interestingly, we observed an increase in RIP1 ubiquitination following the addition of zVAD, suggesting potentially different ubiquitination machinery for RIP1 ubiquitination during necroptosis.

Importantly, inhibiting RIP1 kinase activity by Nec-1 effectively reduced its ubiquitination in the TBZ treatment group (log 2 ratio = 1.66 *versus* control, *P*-value: 0.047), indicating RIP1 ubiquitination during TBZ-induced necroptosis is kinase dependent. To our surprise, Lys115 (K115), one of the ubiquitin conjugation sites on human RIP1, appeared to be differentially regulated compared with the other sites identified on RIP1 (Figures 3d and e). On the one hand, TNF had a minimal effect on K115 ubiquitination level (log 2 ratio = 0.28 *versus* control). On the other hand, BV6 and zVAD treatment in the presence of TNF promoted K115 ubiquitination, which was prevented by Nec-1 treatment (log 2 ratio = 1.39, 2.39 and 0.49 *versus* control, respectively) (Figures 3e and f). We analyzed all Lys sites identified from these experiments and found evolutionarily conserved K115 to be conjugated only in necroptotic conditions (Figures 3f and Supplementary Figure S3B). These data suggest that ubiquitination on Lys115 may be linked with necroptotic cell death and mechanistically different from other RIP1 sites.

Mutation of K115 RIP1 ubiquitination site does not affect inherent RIP1 kinase activity. Lys115 of human RIP1 is located in the kinase domain and structural modeling placed it in the C-terminal portion of kinase domain, away from the active site hinge region (Figure 4a). We purified recombinant kinase domains of RIP1 WT and K115R mutant and assessed their kinase activity *in vitro*. Both WT and K115R RIP1 kinase domain proteins had comparable kinase activity and were inhibited by RIP1 kinase inhibitors Nec-4 and Nec-1Cl to similar extents (Figure 4b). In addition, thermal stability of WT and mutated RIP1 proteins were very similar, suggesting that the biophysical properties of the tested proteins were not changed with the K115R mutation (Figure 4c).

Next, we investigated the effect of the K115R mutation on the full-length RIP1 protein. Ectopic expression of WT, K115R or other lysine-to-arginine mutant RIP1 constructs (identified in our mass spectrometry experiments or previously reported in the literature) showed comparable kinase activity (Figure 4d). To further explore the kinase activity of the RIP1 ubiquitination site mutant, full-length recombinant RIP1 kinase WT, kinase-dead (KD) mutant D138N and K115R were transiently expressed and purified from insect cells (Figure 4e). WT and K115R were phosphorylated to similar degrees upon purification (Figure 4e) and displayed similar kinase activity as measured by an ADP-Glo assay (Promega, Madison, WI, USA) (Figure 4f). Therefore, mutation of K115 residue to R does not affect inherent RIP1 kinase activity.

Necroptotic RIP1 ubiquitination regulates necroptotic cell death signaling. To examine the role of RIP1 ubiquitination for necroptotic signaling, we generated HT29 cells with deletion of RIP1 using the CRISPR/Cas9 system. HT29 RIP1-knockout cells were resistant to TBZ-induced necroptosis, thus functionally validating RIP1 ablation (Figure 5a).[31] Introduction of WT RIP1, but not of KD or K115R RIP1 constructs restored TBZ-stimulated necroptotic cell death in reconstituted HT29 cells (Figures 5a and b). K115R RIP1 mutant was inefficient in mediating necroptotic cell death in HT29 cells and, similarly, reconstitution of immortalized *Rip1*$^{-/-}$ MEFs with K115R or KD RIP1 versions abrogated necroptosis in mouse cells (Supplementary Figure S4A). Furthermore, TBZ-stimulated K63- and linear chain-linked ubiquitination of K115R RIP1 was greatly diminished compared with WT RIP1 (Figure 5c). At the same time, TNF stimulated RIP1 ubiquitination and activation of NF-κB and MAPK signaling, as well as TB-induced apoptotic cell death and caspase-8 processing, was comparable in HT29 or MEF cells reconstituted with K115R or WT RIP1 (Figures 5d–f and Supplementary Figures S4A–D).

Next, we examined if K115R RIP1 could mediate RIP1 phosphorylation during necroptotic signaling. Stimulation with TBZ resulted in robust RIP1 phosphorylation in cells expressing WT RIP1 (Figure 5b). As expected, HT29 cells expressing a KD version of RIP1 did not mediate any RIP1 phosphorylation (Figure 5b). Interestingly, HT29 cells that expressed K115R RIP1 mutant displayed greatly reduced and delayed TBZ-induced RIP1 phosphorylation (Figure 5b). We also investigated whether K115R RIP1 is recruited into the necrosome and found that K115R protein associates with caspase-8 following TBZ treatment (Figure 6a). However, K115R RIP1 found in the necrosome is not phosphorylated, and it is present in reduced amounts compared with WT RIP1 (Figure 6a). Consequently, phosphorylated RIP3 was also found in the complex with WT RIP1 but not K115R RIP1 (Figure 6a). As a consequence of reduced RIP1 phosphorylation and deficient phospho-RIP3 recruitment, we also observed greatly reduced MLKL phosphorylation in K115R RIP1-expressing cells compared with WT RIP1-expressing HT29 cells (Figures 5b and 6a).

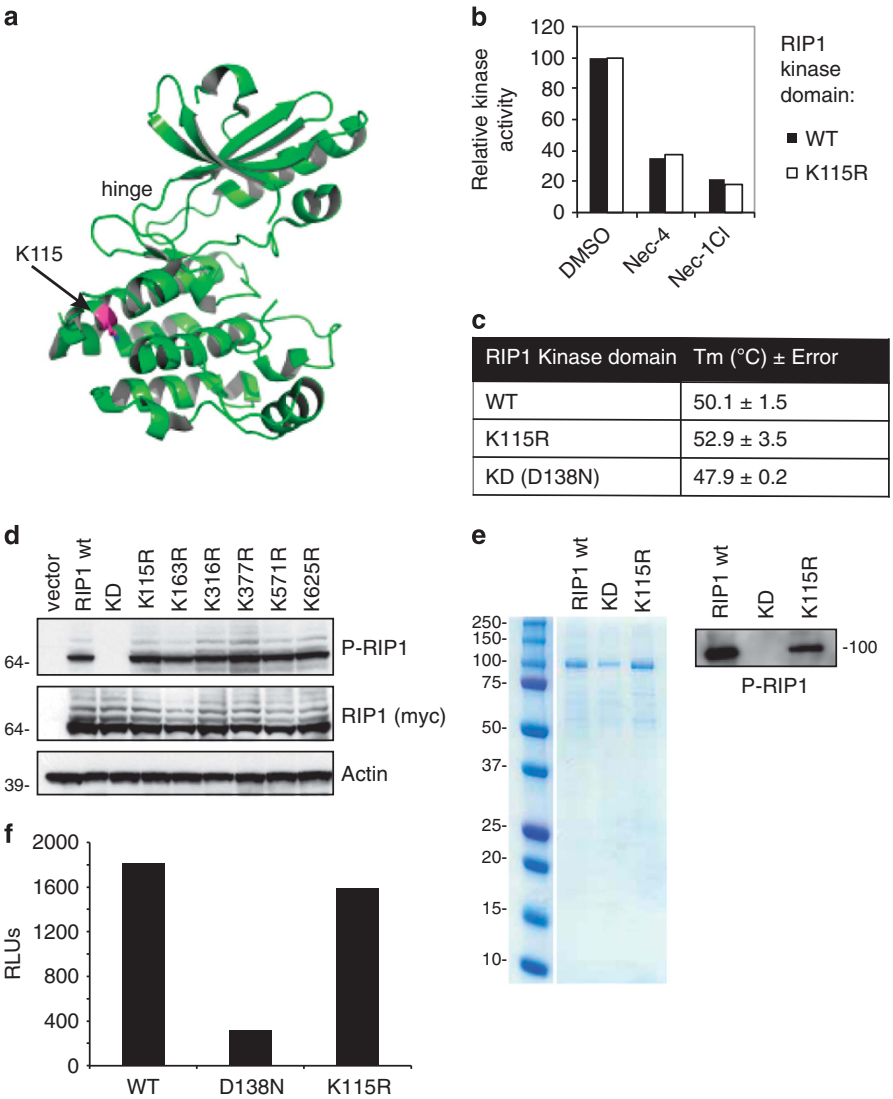

RIP1 Kinase domain	Tm (°C) ± Error
WT	50.1 ± 1.5
K115R	52.9 ± 3.5
KD (D138N)	47.9 ± 0.2

Figure 4 K115R RIP1 ubiquitination site mutant displays inherent kinase activity. (**a**) Crystal structure of RIP1 kinase domain (PDB-ID 4ITJ) illustrating the position of K115 (colored magenta) in the C-terminal domain. (**b**) The kinase activity of recombinant kinase domains of RIP1 WT and K115R proteins can be inhibited by necrostatin compounds as assessed by an HTRF assay. (**c**) Recombinant kinase domain RIP1 WT, KD and K115R proteins were incubated with Sypro orange and submitted to a temperature ramp to assess their thermal stability. Data are mean ± S.E.M. values of three experiments. (**d**) The 293 T cells were transfected with the indicated constructs. After 24 h, cell lysates were analyzed by western blotting with the indicated antibodies. (**e**) Recombinant full-length RIP1 WT, D138N and K115R proteins were expressed in insect cells and purified via Flag resin (Coomassie stain, left side). WT and K115R RIP1 are phosphorylated upon purification. Equal amounts of examined full-length RIP1 proteins were investigated by western blotting with P-RIP1 antibody (right side). (**f**) Full-length WT and K115R RIP1 proteins display similar kinase activity. Kinase activity of equal amounts of examined full-length RIP1 proteins was measured by ADP-Glo assay

Figure 5 Necroptotic RIP1 ubiquitination on Lys115 regulates cell death signaling. (**a**) HT29 RIP1 KO cells reconstituted with the indicated constructs were treated for 24 h with TNFα 20 ng/ml (T), BV6 2 μM (B) and zVAD 20 μM (Z) as indicated. Cell viability was assessed by CellTiter-Glo. Data are mean ± S.E.M. values of three experiments. (**b**) HT29 RIP1 KO (-/-) cells reconstituted with the indicated constructs were treated as in (**a**) for 0, 1, 2 or 4 h. Cell lysates were analyzed by western blotting with the indicated antibodies. (**c**) Reduced necroptotic ubiquitination in HT29 cells expressing K115R RIP1. WT or K115R RIP1 HT29 cells were treated with TBZ for 2 h as in (**a**). Cells were lysed in 6 M urea buffer, immunoprecipitated using linear or K63 linkage-specific anti-ubiquitin antibodies and analyzed by western blotting with the indicated antibodies. (**d**) K115 RIP1 ubiquitination is not critical for TNF-associated RIP1 ubiquitination. HT29 RIP1 KO cells reconstituted with vector, RIP1 WT or RIP1 K115R constructs were treated for 7 min with Flag-TNFα 20 ng/ml and cell lysates were immunoprecipitated with Flag-TNF. The pull-downs and cell lysates were analyzed by western blotting with the indicated antibodies. (**e** and **f**) K115 RIP1 ubiquitination is not critical for TNF-induced NF-κB and MAPK signaling in HT29 cells. (**e**) HT29 RIP1 KO cells reconstituted with vector, RIP1 WT or RIP1 K115R constructs were treated for indicated time points with TNFα 20 ng/ml for 4 h and IL-8 mRNA levels were examined by quantitative real-time PCR. (**f**) HT29 RIP1 KO cells reconstituted with vector, RIP1 WT or RIP1 K115R constructs were treated for indicated time points with TNFα 20 ng/ml and cell lysates were analyzed by western blotting with the indicated antibodies

We have additionally investigated the assembly of necroptotic cell death complexes in RIP1-null HT29 cells expressing vector, WT or K115R RIP1 by using gel filtration (Figure 6b). Expression of WT RIP1 allowed efficient translocation of ubiquitinated and phosphorylated RIP1, as well as phosphorylated RIP3 and MLKL, into large protein complexes (Figure 6b). On the other hand, expression of K115R RIP1 prohibited accumulation of ubiquitinated and phosphorylated RIP1, RIP3 and MLKL (Figure 6b).

Thus, abrogation of necroptotic RIP1 ubiquitination disrupts RIP1 phosphorylation, which is essential for necroptotic cell death. Finally, we investigated the ability of WT or K115R RIP1-expressing HT29 cells to mediate secretion of necroptosis-associated inflammatory DAMP HMGB1.

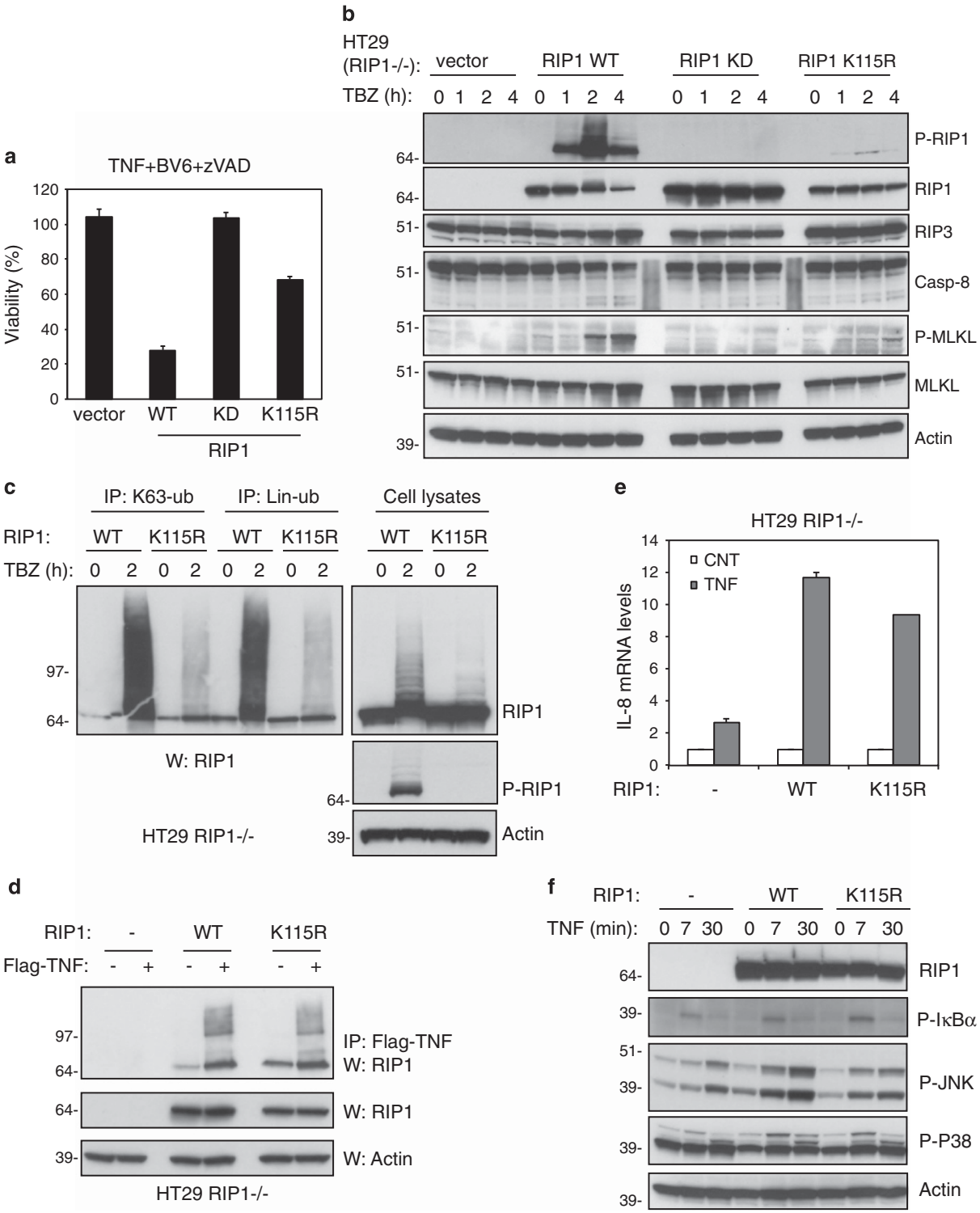

K115R RIP1-expressing cells secreted reduced amount of HMGB1 in accordance with diminished necroptotic capacity of ubiquitination-compromised K115R form of RIP1 (Supplementary Figure S4E). Therefore, these data suggest that necroptotic ubiquitination allows accumulation of phosphorylated RIP1 and RIP3 and stabilizes RIP1 in the necrosome, thus allowing efficient RIP1 kinase activity and mediation of necroptotic signaling.

RIP1 ubiquitination in kidneys undergoing ischemia–reperfusion injury. Previous work by Andreas Linkermann and a recent study from our group have demonstrated the importance of RIP1 kinase activity in ischemia–reperfusion kidney injury.[32,33] We have investigated kidney damage following ischemia–reperfusion injury (IRI) by examining the blood serum creatinine and blood urea nitrogen (BUN) levels 24 h following the procedure (Supplementary Figure S5A). We observed high BUN and creatinine levels in a couple of animals 24 h postprocedure (Supplementary Figure S5A). Kidneys harvested from tested animals were dissolved in lysis buffer and examined by western blotting (Supplementary Figure S5B). Interestingly, we observed noticeable RIP1 ubiquitination in a couple of 24 h kidney samples that also showed high levels of BUN and creatinine (Supplementary Figures S5A and B). Kidney sections from the 24 h group were stained with hematoxylin and eosin to evaluate the extent of tissue damage. Sections that had high levels of BUN and creatinine (samples 4 and 6) showed prominent RIP1 ubiquitination as well as extensive necrotic areas (Supplementary Figure S5C), suggesting that RIP1 ubiquitination occurs in damaged kidneys that undergo IRI.

Discussion

Precise regulation of post-translational protein modifications have an important role in fine-tuning many cellular processes such as cell division, proliferation and survival. Phosphorylation, ubiquitination, sumoylation and neddylation of a number of cell death regulators have been reported to be critical for the execution or inhibition of cellular death.[25,34] Necroptosis is a regulated form of cell death that relies on the kinase activity of RIP1 and RIP3.[5,19,35] Although the phosphorylation of RIP1 and RIP3, as well as of the RIP3 substrate MLKL, is well documented and studied, the roles of other post-translational modifications in this pathway are less understood. Two recent studies reported necroptotic RIP1 and RIP3 ubiquitination, but the functional role of these ubiquitination events during necroptotic signaling was not clear.[26,27,29] Here we provide evidence that necroptotic RIP1 ubiquitination is relevant for the execution of necroptotic cell death. However, necroptotic cell death is not required as necroptotic RIP1 ubiquitination occurs in the absence of necroptotic executors RIP3 and MLKL or when RIP3 kinase activity is inhibited. Instead, RIP1 ubiquitination takes place in the necrosome complex independent of RIP3.

Interestingly, necroptotic RIP1 phosphorylation and ubiquitination seem to be tightly coordinated: inhibition or absence of RIP1 kinase activity blocks necroptotic RIP1 ubiquitination, whereas mutation of RIP1 necroptosis-associated ubiquitination site (K115R) dampens RIP1 kinase activity during necroptotic signaling. Given that only kinase-capable RIP1 protein associates with the necrosome[30,31] and that necroptotic RIP1 ubiquitination occurs in the necrosome, it is not surprising that RIP1 kinase activity has such deterministic role for necroptotic RIP1 ubiquitination. On the other hand, the influence of necroptotic RIP1 ubiquitination on RIP1 kinase activity is more enigmatic. Mutation of K115 to R should not perturb overall conformation of RIP1 and it does not deprive RIP1 of its inherent kinase activity. Nevertheless, K115R RIP1 mutant shows greatly decreased kinase activity and inability to accumulate and stabilize within the necrosome complex, which, consequently, leads to diminished ability to mediate necroptotic cell death. We hypothesize that RIP1 ubiquitination stabilizes RIP1 within the necrosome, thus enhancing its kinase activity. Structural studies of ubiquitinated RIP1 in complex with RIP3 and caspase-8 are likely needed to provide full molecular details of these signaling events.

Our proteomic profiling of ubiquitination events during necroptosis has revealed that necroptosis signaling indeed promotes a pathway-specific profile of ubiquitination, with RIP1 being the most prominent target. However, there are a number of additional proteins whose ubiquitination status changes during necroptosis signaling, and thus we believe that future studies will expose functional relevance of those modifications and enhance the complexity and understanding of necroptotic pathways. Finally, necroptotic RIP1 ubiquitination takes place *in vivo* as well, as we observed intense RIP1 ubiquitination in damaged kidneys. Although it is not yet clear how IRI of kidneys leads to the activation of RIP1-mediated necroptosis, RIP1 kinase activity has an instrumental role in this process as an RIP1 kinase inhibitor or kinase-inactive RIP1 efficiently block IRI-induced kidney damage.[32,33] Given that RIP1 ubiquitination takes place in highly damaged kidneys, it is possible to envision that RIP1 ubiquitination might serve as an additional biomarker for this pathology. In summary, this study reveals coordinated and interdependent RIP1 phosphorylation and ubiquitination within the necroptotic complex that regulates necroptotic signaling, tissue damage and cell death.

Materials and Methods

Reagents and transfections. The following materials have been used: human recombinant soluble TNFα (Genentech, South San Francisco, CA, USA), mouse recombinant soluble TNFα (R&D, Minneapolis, MN, USA), Flag-TNFα (Enzo, Life Sciences, Farmingdale, NY, USA), zVAD-Fmk (MBL, Woburn, MA, USA), Nec-1 (Sigma, St. Louis, MO, USA), BV6, Nec-1a, Nec-4, Nec-1Cl, GSK843[36–38] (all synthesized at Genentech). The primary antibodies used were directed against: RIP1, FADD, JNK (Jun N-terminal kinase), P-JNK, P-ERK (BD Biosciences), human and mouse RIP3 (Imgenex, Littleton, CO, USA, Genentech and Cell Signaling, Danvers, MA, USA), human c-IAP1 and mouse pan-c-IAP (R&D), human c-IAP2 (Novus, Littleton, CO, USA), actin (Sigma), mouse FADD (Santa Cruz Biotechnology, Santa Cruz, CA, USA and Genentech), ubiquitin (P4D1; Cell Signaling), anti-human P-RIP1 antibody raised against S166 of human RIP1 (Cell Signaling), IκBα, P-IκBα, P-p38, Hsp90 (Cell Signaling), human caspase-8 (Cell signaling and Enzo), mouse caspase-8, mouse c-IAP1 (Enzo), Myc, K63 and linear ubiquitin chains (Genentech), MLKL (Millipore, Billerica, MA, USA), P-RIP3 and P-MLKL (Abcam, Cambridge, MA, USA), FLAG-HRP conjugate (Sigma). Plasmid transfections were carried out using Fugene 6 (Promega) for 24 or 48 h.

Cell lines. Human colon carcinoma HT29, fibrosarcoma HT1080 and embryonic kidney 293 T cell lines were obtained from the American Type Culture Collection (ATCC, Manassas, VA, USA). HT29 RIP1$^{-/-}$ cells were produced by CRISPR with the probes hRIP1_2, 5′-GGGTGTATTTCCTAGATAGTTGG-3′ and hRIP1_3, 5′-

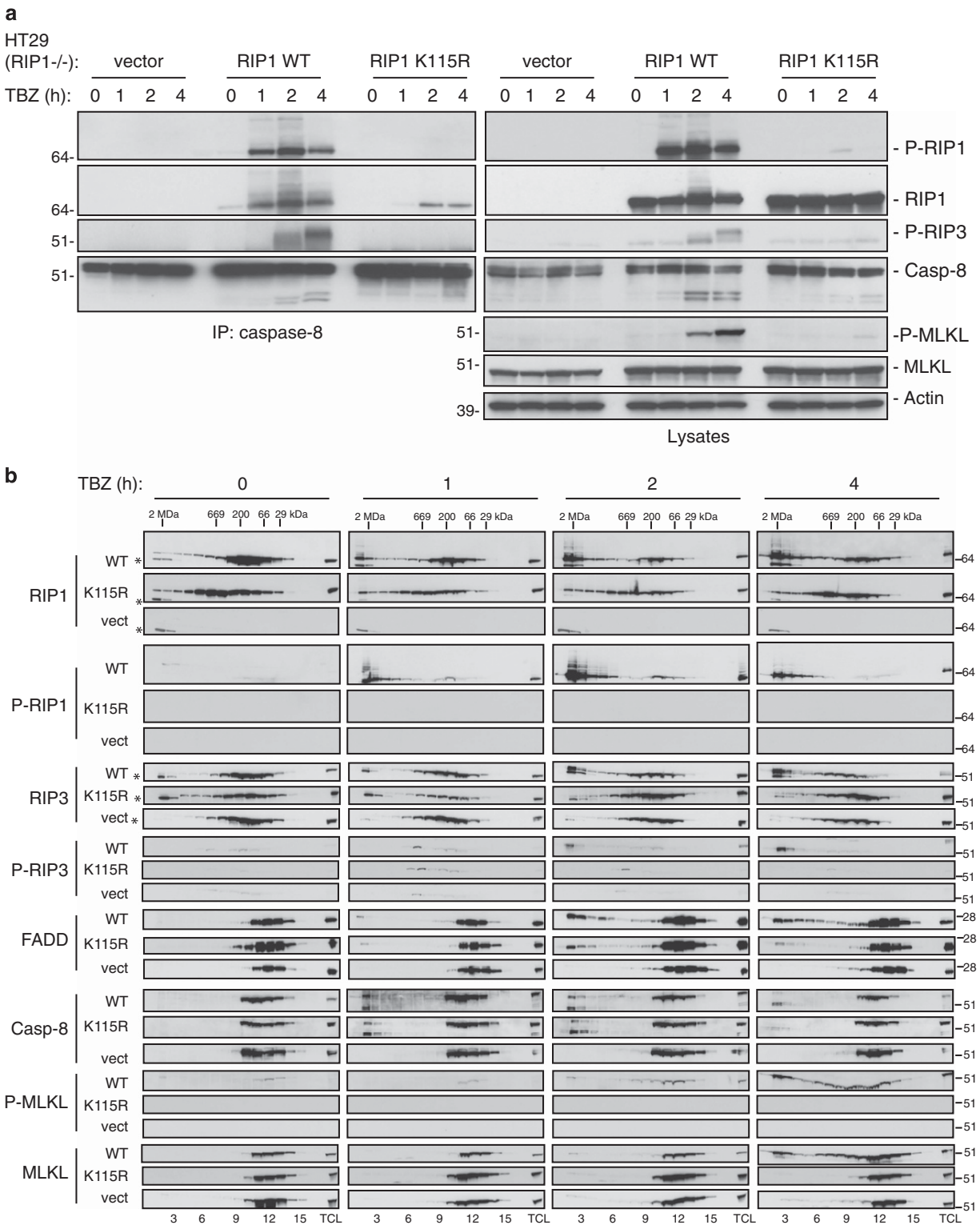

Figure 6 Necroptotic RIP1 ubiquitination on Lys115 regulates necrosome assembly. (**a**) HT29 RIP1 KO (-/-) cells reconstituted with vector, WT RIP1 or K115R RIP1 constructs were treated TNFα 20 ng/ml (T), BV6 2 μM (B) and zVAD 20 μM (Z) for indicated time points. Cell lysates were immunoprecipitated with caspase-8 antibody. The pull-downs and lysates were analyzed by western blotting with the indicated antibodies. (**b**) Gel filtration analysis of the necrosome. HT29 RIP1 KO cells reconstituted with vector, WT RIP1 or K115R RIP1 constructs were treated as in (**a**) for the indicated times. Lysates were fractionated on a Superose 6 10/300 GL column and the resulting fractions as well as total cell lysate were separated by SDS-PAGE and probed with the indicated antibodies. Asterisks denote nonspecific bands. Fraction numbers are indicated below and molecular weight markers on top of western blots

TAATGCTGAGGAAGAAGTACCGG-3′. HT29 RIP1 stably reconstituted cells were produced by retrovirus transduction of Myc-RIP1 constructs and selected in 1.5 μg/ml puromycin. Cells were grown and maintained in 50 : 50 F12/DMEM medium supplemented with 10% fetal bovine serum, penicillin, streptomycin and 2 mM glutamine at 5% CO_2. WT and RIP1$^{-/-}$, RIP1-KD-KI, RIP3$^{-/-}$ and MLKL$^{-/-}$ MEFs[21] were cultured in DMEM medium supplemented with 10% heat-inactivated serum, penicillin, streptomycin, 2 mM glutamine and non-essential amino acids at 5% CO_2. RIP1$^{-/-}$ MEFs immortalized with E1A were stably reconstituted with RIP1 by retrovirus transduction of Flag-RIP1 constructs and selected in 1 μg/ml puromycin. Primary MEFs were cultured in DMEM medium supplemented with 10% heat-inactivated serum, penicillin, streptomycin, 2 mM glutamine and β-mercaptoethanol at 5% CO_2 in 0.1% gelatin-precoated plates. Primary bone marrow-derived macrophages (BMDMs) were obtained from mouse rear leg's bone marrow and differentiated to macrophages for 1 week with M-CSF. BMDM medium was supplemented with 10 mM HEPES and 25 ng/ml M-CSF.

Viability assays. Cell viability was assessed using Cell TiterGlo (Promega) following the manufacturer's specifications.

Western blot analysis and immunoprecipitation. Western blot analyses and immunoprecipitations were performed with the following lysis buffer: 20 mM Tris-HCl (pH 7.5), 150 mM NaCl, 1 mM EDTA, 1% Triton X-100, 1 mM PMSF, Halt Protease and Phosphatase Inhibitor Cocktail (Thermo Scientific, San Jose, CA, USA). Cells were lysed on ice for 30 min and centrifuged at 14 000 r.p.m. for 10 min at 4 °C. General immunoprecipitations and ubiquitin chain-specific immunoprecipitations were performed as described recently.[26,39]

Gel filtration. HT29 cells were treated with 20 ng/ml TNF, 2 μM BV6 and 20 μM zVAD for the indicated times. Cells were lysed in the same buffer as for western blot analyses and lysates were separated on a Superose 6 10/300 GL column (GE Healthcare, Little Chalfont, UK). Fractions of 1 ml were collected and precipitated with deoxycholic acid and trichloroacetic acid. The resulting pellets were washed with acetone and resuspended in 2x LDS sample buffer (Novex, Waltham, MA, USA). Fractions and 50 μg total cell lysate were separated on 4–12% Bis-Tris gels (Bio-Rad, Hercules, CA, USA) and probed with the indicated antibodies. Molecular weight markers (Sigma-Aldrich, St. Louis, MO, USA) were run before the samples for column calibration.

K-GG immunoaffinity enrichment and mass spectrometry analysis. Immunoaffinity enrichment of K-GG (Lys-Gly-Gly) peptides and LiME (linear mixed-effects) analysis were carried out as described previously.[40] Immunoaffinity enrichment of K-GG peptides was carried out using PTMscan reagents and protocols (Cell Signaling Technology). Cells were lysed under denaturing conditions (9 M urea and 20 mM HEPES, pH 8.0). Protein amount was quantified using the Bradford assay. From each sample, 40 mg of lysate proteins were reduced with dithiothreitol (DTT) and alkylated with iodoacetemide. Clarified lysates were then diluted to a final concentration of 2 M urea and digested overnight at 37 °C with trypsin. Digested peptides were desalted using SepPak C18 cartridges (Waters, Milford, MA, USA) and then lyophilized for $>$ 48 h. Dry peptides were reconstituted in IAP buffer and incubated with anti-K-GG-coupled resin for 2 h at 4 °C. Resins were washed two times with IAP buffer and four times with water before elution in 0.15% TFA (trifluoroacetic acid) (two times for 10 min each). Enriched peptides were prepared for MS analysis using standard protocol for C18 STAGE tips,[41] with elution performed in 60% acetonitrile/0.1% TFA. Samples were dried completely. All peptides were analyzed with a NanoAcquity UPLC system (Waters) directly coupled to an LTQ Orbitrap Elite mass spectrometer (Thermo Scientific). Peptides were reconstituted in 0.1% formic acid (FA) with 2% acetonitrile (ACN), loaded onto a Symmetry C18 column (1.7 mm BEH-130, 0.1 x 100 mm^2; Waters) and separated with a 60-min gradient from 0 to 15%, 0 to 20% or 2 to 25% solvent B (0.1% FA, 98% ACN) at 1 μl/min flow rate. Peptides were eluted directly into the mass spectrometer with a spray voltage of 1.2 kV. Full MS data were acquired in FT for 375–1600 *m/z* with a 60 000 resolution. The 15 most abundant ions found in the full MS were selected for MS/MS through a 2-Da isolation window.

Peptide spectral matching, ubiquitination site localization and quantification. Mass spectral data were analyzed as described previously[40,42,43] using a combination of in-house tools and publicly available algorithms. Searches were performed against a concatenated target-decoy database containing Uniprot human protein sequences (version 2011_12) and common contaminants (119 247 entries) with Mascot (Matrix Science, Boston, MA, USA; version 2.3.02). Search criteria included a full MS tolerance of 50 p.p.m., MS/MS tolerance of 0.8 Da with oxidation (+15.9949 Da) of methionine and ubiquitination (+114.0429 Da) of lysine as variable modifications and carbamidomethylation (+57.0215 Da) of cysteine as static modifications. PSMs were filtered to a peptide false discovery rate (FDR) of 5% using a linear discriminant analysis on a per-run basis. In aggregate, the data were filtered to a 2% protein FDR. Site localization scores were determined for confidently identified K-GG peptides using a modified version of the AScore algorithm.[44]

Quantification of peak areas corresponding to K-GG-modified peptides was performed using the VistaGrande XQuant algorithm.[45,46] XQuant results were filtered to a confidence score of 83 or greater and exported for further processing and graphical analysis using mixed-effect modeling. Area under the curve (AUC) peak areas were of median intensity and normalized on the run-to-run basis. A mixed-effect model was fit to the AUC for each protein on a per-experiment basis, with 'Treatment' set as a categorical fixed effect and 'Peptide' fit as a random effect using the 'nlme' package (version 3.1-118).

***In vitro* kinase assay.** *HTRF assay*: The kinase activity was assessed using HTRF KinEASE Substrate 3 (Cisbio Bioassays, Bedford, MA, USA) for 3 h at 30 °C following manufacturer's specifications. Briefly, 200 ng of RIP1 kinase domain were incubated in Buffer 1x (in which DTT, $MnCl_2$ and $MgCl_2$ were added) with 2 μM of substrate, 250 μM ATP, 125 nM streptavidin-XL665 and substrate Eu^{3+}-Cryptate antibody.

ADP-Glo (Promega) assay was used according to the manufacturer's specifications.

Recombinant proteins. Recombinant RIP1-EGFP-Flag proteins were transiently expressed in Sf9 cells using Mirus TransIT reagent (Madison, WI, USA) for insect cell transfection. Cells were harvested 3 days after transfection and lysed in 50 mM Tris (pH 8), 300 mM NaCl, 10% glycerol, 0.002% Brij-35, 1 mM DTT and protease inhibitor tablets. Cells were lysed by sonication and RIP1 was purified via the C-terminal Flag-tag on Flag resin. Protein purity was assessed by mass spectrometry, which did not identify any protein other than RIP1.

His-tagged human RIP1 kinase domain proteins were produced in Sf9 insect cells by baculovirus transduction. Cells were lysed with 50 mM Tris (pH 8.0), 300 mM NaCl, 20 mM imidazole, 1 mM tris-2 carboxy ethylphosphine (TCEP) and protease inhibitor cocktail (Roche, Indianapolis, IN, USA). His-RIP1 kinase domain was purified using Ni-NTA resin with buffer A: 20 mM Tris (pH 8.0), 300 mM NaCl, 20 mM imidazole and 0.5 mM TCEP. Proteins were eluted from Ni-NTA column by buffer A +250 mM imidazole. The eluted proteins were purified by FPLC on a Superdex 200 column using: 20 mM Tris (pH 7.5), 150 mM NaCl, 5% glycerol and 0.5 mM TCEP. The selected fractions were pooled and concentrated.

Thermal stability. One microgram of baculovirus produced human RIP1 kinase domain; WT, K115R and KD were incubated with Sypro Orange (Sigma) diluted in protein buffer 1/2000, in a final reaction volume of 20 μl. The sample was submitted to a heat ramp from 25 °C to 95 °C in a PCR Real Time machine (Thermofisher, Waltham, MA, USA).

ELISA. The presence of HMGB1 protein in the supernatant of treated cells was assessed using HMGB1 ELISA (LifeSpan Biosciences, Seattle, WA, USA) following the manufacturer's specifications.

Kidney IRI. Kidney IRI was performed as described previously.[32] Briefly, both left and right renal pedicles of male mice aged 9–11 weeks were clamped for 30 min under anesthesia. Following the wound closure, mice received 0.5 ml sterile saline intraperitoneally and were allowed to recover. All animal protocols were approved by the Genentech animal care and use committee.

Real-time quantitative PCR and siRNAs. RNA was isolated from cells with the RNeasy Mini Kit (Qiagen) following standard protocols. An on-column DNase treatment was included. cDNA was generated from each RNA sample using a Taqman Gene Expression Cells to Ct Kit (Life Technologies, Waltham, MA, USA). Gene expression assay for interleukin-8 (IL-8) (Hs00174103_m1) and GAPDH (Hs03929097_g1) were from Life Technologies. IL-8 levels were normalized against GAPDH gene expression. The sequences of siRNA oligos targeting human RIP3 are: 5′-GGAATGCCTACCAAAAACTTT-3′ and 5′-GGCCACAGGGTTGGTATAATT-3′, and for human MLKL: 5′-TGAGTTACCAGGAAGTTTGTT-3′.

Conflict of Interest

MCdA and MK are former and all other authors are current employees of Genentech. The authors declare no conflict of interest.

Acknowledgements. We thank Kerry Zobel, Kurt Deshayes, Wayne J Fairbrother, Vishva M Dixit, Adam Johnson, Snahel Patel, Alberto Estevez, Bobby Brillantes, Ben Haley, members of the Early Discovery Biochemistry department and the Oligo Synthesis and Sequencing facilities at Genentech that provided help with insightful discussions, suggestions and reagents.

1. Steller H. Mechanisms and genes of cellular suicide. *Science* 1995; **267**: 1445–1449.
2. Linkermann A, Stockwell BR, Krautwald S, Anders HJ. Regulated cell death and inflammation: an auto-amplification loop causes organ failure. *Nat Rev Immunol* 2014; **14**: 759–767.
3. Salvesen GS, Abrams JM. Caspase activation – stepping on the gas or releasing the brakes? Lessons from humans and flies. *Oncogene* 2004; **23**: 2774–2784.
4. Linkermann A, Green DR. Necroptosis. *N Engl J Med* 2014; **370**: 455–465.
5. Newton K. RIPK1 and RIPK3: critical regulators of inflammation and cell death. *Trends Cell Biol* 2015; **25**: 347–353.
6. Vanden Berghe T, Linkermann A, Jouan-Lanhouet S, Walczak H, Vandenabeele P. Regulated necrosis: the expanding network of non-apoptotic cell death pathways. *Nat Rev Mol Cell Biol* 2014; **15**: 135–147.
7. Silke J, Brink R. Regulation of TNFRSF and innate immune signalling complexes by TRAFs and cIAPs. *Cell Death Differ* 2010; **17**: 35–45.
8. Varfolomeev E, Goncharov T, Fedorova AV, Dynek JN, Zobel K, Deshayes K *et al.* c-IAP1 and c-IAP2 are critical mediators of tumor necrosis factor alpha (TNFα)-induced NF-κB activation. *J Biol Chem* 2008; **283**: 24295–24299.
9. Haas TL, Emmerich CH, Gerlach B, Schmukle AC, Cordier SM, Rieser E *et al.* Recruitment of the linear ubiquitin chain assembly complex stabilizes the TNF-R1 signaling complex and is required for TNF-mediated gene induction. *Mol Cell* 2009; **36**: 831–844.
10. Varfolomeev E, Goncharov T, Maecker H, Zobel K, Komuves LG, Deshayes K *et al.* Cellular inhibitors of apoptosis are global regulators of NF-kappaB and MAPK activation by members of the TNF family of receptors. *Sci Signal* 2012; **5**: ra22.
11. Tokunaga F. Linear ubiquitination-mediated NF-kappaB regulation and its related disorders. *J Biochem* 2013; **154**: 313–323.
12. Dynek JN, Goncharov T, Dueber EC, Fedorova AV, Izrael-Tomasevic A, Phu L *et al.* c-IAP1 and UbcH5 promote K11-linked polyubiquitination of RIP1 in TNF signalling. *EMBO J* 2010; **29**: 4198–4209.
13. Gerlach B, Cordier SM, Schmukle AC, Emmerich CH, Rieser E, Haas TL *et al.* Linear ubiquitination prevents inflammation and regulates immune signalling. *Nature* 2011; **471**: 591–596.
14. Silke J, Vucic D. IAP family of cell death and signaling regulators. *Methods Enzymol* 2014; **545**: 35–65.
15. Sun L, Wang H, Wang Z, He S, Chen S, Liao D *et al.* Mixed lineage kinase domain-like protein mediates necrosis signaling downstream of RIP3 kinase. *Cell* 2012; **148**: 213–227.
16. Zhao J, Jitkaew S, Cai Z, Choksi S, Li Q, Luo J *et al.* Mixed lineage kinase domain-like is a key receptor interacting protein 3 downstream component of TNF-induced necrosis. *Proc Natl Acad Sci USA* 2012; **109**: 5322–5327.
17. Dondelinger Y, Declercq W, Montessuit S, Roelandt R, Goncalves A, Bruggeman I *et al.* MLKL compromises plasma membrane integrity by binding to phosphatidylinositol phosphates. *Cell Rep* 2014; **7**: 971–981.
18. Murphy JM, Czabotar PE, Hildebrand JM, Lucet IS, Zhang JG, Alvarez-Diaz S *et al.* The pseudokinase MLKL mediates necroptosis via a molecular switch mechanism. *Immunity* 2013; **39**: 443–453.
19. Oberst A. Death in the fast lane: what's next for necroptosis? *FEBS J* 2015; **283**: 2616–2625.
20. Kaiser WJ, Daley-Bauer LP, Thapa RJ, Mandal P, Berger SB, Huang C *et al.* RIP1 suppresses innate immune necrotic as well as apoptotic cell death during mammalian parturition. *Proc Natl Acad Sci USA* 2014; **111**: 7753–7758.
21. Newton K, Dugger DL, Wickliffe KE, Kapoor N, de Almagro MC, Vucic D *et al.* Activity of protein kinase RIPK3 determines whether cells die by necroptosis or apoptosis. *Science* 2014; **343**: 1357–1360.
22. Hershko A, Ciechanover A. The ubiquitin system. *Annu Rev Biochem* 1998; **67**: 425–479.
23. Ikeda F, Dikic I. Atypical ubiquitin chains: new molecular signals. 'Protein Modifications: Beyond the Usual Suspects' review series. *EMBO Rep* 2008; **9**: 536–542.
24. Peltzer N, Darding M, Walczak H. Holding RIPK1 on the ubiquitin leash in TNFR1 signaling. *Trends Cell Biol* 2016; **26**: 445–461.
25. Vucic D, Dixit VM, Wertz IE. Ubiquitylation in apoptosis: a post-translational modification at the edge of life and death. *Nat Rev Mol Cell Biol* 2011; **12**: 439–452.
26. de Almagro MC, Goncharov T, Newton K, Vucic D. Cellular IAP proteins and LUBAC differentially regulate necrosome-associated RIP1 ubiquitination. *Cell Death Dis* 2015; **6**: e1800.
27. Lawlor KE, Khan N, Mildenhall A, Gerlic M, Croker BA, D'Cruz AA *et al.* RIPK3 promotes cell death and NLRP3 inflammasome activation in the absence of MLKL. *Nat Commun* 2015; **6**: 6282.
28. Moriwaki K, Chan FK. Regulation of RIPK3 and RHIM-dependent necroptosis by the proteasome. *J Biol Chem* 2016; **291**: 5948–5959.
29. Dondelinger Y, Darding M, Bertrand MJ, Walczak H. Poly-ubiquitination in TNFR1-mediated necroptosis. *Cell Mol Life Sci* 2016; **73**: 2165–2176.
30. Cho YS, Challa S, Moquin D, Genga R, Ray TD, Guildford M *et al.* Phosphorylation-driven assembly of the RIP1-RIP3 complex regulates programmed necrosis and virus-induced inflammation. *Cell* 2009; **137**: 1112–1123.
31. He S, Wang L, Miao L, Wang T, Du F, Zhao L *et al.* Receptor interacting protein kinase-3 determines cellular necrotic response to TNF-alpha. *Cell* 2009; **137**: 1100–1111.
32. Linkermann A, Brasen JH, Himmerkus N, Liu S, Huber TB, Kunzendorf U *et al.* Rip1 (receptor-interacting protein kinase 1) mediates necroptosis and contributes to renal ischemia/reperfusion injury. *Kidney Int* 2012; **81**: 751–761.
33. Newton K, Dugger DL, Maltzman A, Greve JM, Hedehus M, Martin-McNulty B *et al.* RIPK3 deficiency or catalytically inactive RIPK1 provides greater benefit than MLKL deficiency in mouse models of inflammation and tissue injury. *Cell Death Differ* 2016 (e-pub ahead of print 13 May 2016; doi:10.1038/cdd.2016.46).
34. Popovic D, Vucic D, Dikic I. Ubiquitination in disease pathogenesis and treatment. *Nat Med* 2014; **20**: 1242–1253.
35. Mocarski ES, Upton JW, Kaiser WJ. Viral infection and the evolution of caspase 8-regulated apoptotic and necrotic death pathways. *Nat Rev Immunol* 2012; **12**: 79–88.
36. Takahashi N, Duprez L, Grootjans S, Cauwels A, Nerinckx W, DuHadaway JB *et al.* Necrostatin-1 analogues: critical issues on the specificity, activity and *in vivo* use in experimental disease models. *Cell Death Dis* 2012; **3**: e437.
37. Mandal P, Berger SB, Pillay S, Moriwaki K, Huang C, Guo H *et al.* RIP3 induces apoptosis independent of pronecrotic kinase activity. *Mol Cell* 2014; **56**: 481–495.
38. Varfolomeev E, Blankenship JW, Wayson SM, Fedorova AV, Kayagaki N, Garg P *et al.* IAP antagonists induce autoubiquitination of c-IAPs, NF-κB activation, and TNFα-dependent apoptosis. *Cell* 2007; **131**: 669–681.
39. Goncharov T, Niessen K, de Almagro MC, Izrael-Tomasevic A, Fedorova AV, Varfolomeev E *et al.* OTUB1 modulates c-IAP1 stability to regulate signalling pathways. *EMBO J* 2013; **32**: 1103–1114.
40. Varfolomeev E, Izrael-Tomasevic A, Yu K, Bustos D, Goncharov T, Belmont LD *et al.* Ubiquitination profiling identifies sensitivity factors for IAP antagonist treatment. *Biochem J* 2015; **466**: 45–54.
41. Rappsilber J, Ishihama Y, Mann M. Stop and go extraction tips for matrix-assisted laser desorption/ionization, nanoelectrospray, and LC/MS sample pretreatment in proteomics. *Anal Chem* 2003; **75**: 663–670.
42. Yu K, Phu L, Varfolomeev E, Bustos D, Vucic D, Kirkpatrick DS. Immunoaffinity enrichment coupled to quantitative mass spectrometry reveals ubiquitin-mediated signaling events. *J Mol Biol* 2015; **427**: 2121–2134.
43. Anania VG, Pham VC, Huang X, Masselot A, Lill JR, Kirkpatrick DS. Peptide level immunoaffinity enrichment enhances ubiquitination site identification on individual proteins. *Mol Cell Proteomics* 2014; **13**: 145–156.
44. Beausoleil SA, Villen J, Gerber SA, Rush J, Gygi SP. A probability-based approach for high-throughput protein phosphorylation analysis and site localization. *Nat Biotechnol* 2006; **24**: 1285–1292.
45. Bakalarski CE, Elias JE, Villen J, Haas W, Gerber SA, Everley PA *et al.* The impact of peptide abundance and dynamic range on stable-isotope-based quantitative proteomic analyses. *J Proteome Res* 2008; **7**: 4756–4765.
46. Kirkpatrick DS, Bustos DJ, Dogan T, Chan J, Phu L, Young A *et al.* Phosphoproteomic characterization of DNA damage response in melanoma cells following MEK/PI3K dual inhibition. *Proc Natl Acad Sci USA* 2013; **110**: 19426–19431.

Supplementary Information accompanies this paper on Cell Death and Differentiation website (http://www.nature.com/cdd)